



Comparison of the mechanical characteristics of engineered and waste steel fiber used as reinforcement for concrete



Jacek Domski ^a, Jacek Katzer ^{a,*}, Mateusz Zakrzewski ^a, Tomasz Ponikiewski ^b

^a Faculty of Civil Engineering, Environmental and Geodetic Sciences, Koszalin University of Technology, Koszalin, Poland

^b Faculty of Civil Engineering, Silesian University of Technology, Gliwice, Poland

ARTICLE INFO

Article history:

Received 14 November 2016

Received in revised form

26 April 2017

Accepted 28 April 2017

Keywords:

Waste

Fibre

Tyre

Concrete

SFRC

Reinforcement

ABSTRACT

Engineered steel fiber has been used for reinforcing concrete since the mid-nineteenth century. The influence of fiber reinforcement on the mechanical characteristics of concrete is commonly known and thoroughly described in literature. The fast growing and vibrant market of engineered steel fiber is increasingly disrupted by waste steel fiber obtained during recycling of tires. The lack of knowledge about properties of the waste steel fiber significantly limits its technically viable use. The main aim of the conducted research program was to test waste steel fiber and to compare its properties with most popular engineered steel fiber. Such properties as tensile strength estimated according to EN ISO 6892-1:2009, ductility tested according to EN 10218-1:1994, and tensile strength after ductility test were considered. Waste steel fiber proved to be characterized by much higher tensile strength and ductility than engineered steel fiber. Stress–strain characteristics of both the types of fiber also differ significantly. Conducted bends influence the tensile strength and modulus of elasticity of all tested waste and engineered steel fiber. The achieved knowledge would allow to create sustainable steel fiber-reinforced concretes in a much more efficient way.

© 2017 Published by Elsevier Ltd.

1. Introduction

Fiber-reinforced construction materials have been known since ancient times. In Pharaohs' Egypt mud bricks were reinforced by straw. Romans used a whole range of different fiber of organic origin to modify brittle clay bricks and lime mortars (Maidl, 1995). When modern concrete was born at the beginning of the nineteenth century, its brittleness forced engineers to look for a new type of reinforcement (Nawy, 1996). Steel bars, stirrups, meshes, mats and fibers were the answer to this challenge. Steel fiber-reinforced concrete (SFRC) was one of the very earliest modern structural materials (Havlikova et al., 2015). In the early twentieth century, first engineered fibers for concrete reinforcement were produced in different shapes and sizes. Over the years some geometrical fiber shapes proved to be easy to produce and practical to use (Spinella, 2013). Others did not catch up and were abandoned (Katzer, 2006). Currently, there are dozens of major producers of engineered steel fiber (ESF) located all over the world (Katzer and Domski, 2012). Altogether they offer hundreds of steel

fiber types differentiated by geometric shape, size, diameter, and finishing of surface (Naaman, 2003).

The global market of steel fiber is assessed at 300,000 tons of ESF sold per year and is growing very fast with a rate of 20% per year (Pająk and Ponikiewski, 2013). Over 90% of the steel fiber available on the market is ESF with deformed ends, treated surface, twisted, crimped, and hooked (see Fig. 1.) (Mohammadi et al., 2008). In the past 15 years, the ESF market has been increasingly disrupted by waste steel fiber (WSF) obtained during recycling of tires (Ghorpade and Sudarsana Rao, 2010). Worldwide, over one billion of fully exploited tires arise annually (Graeff et al., 2012). So far, majority of these tires have been disposed to landfill (Pilakoutas et al., 2004). Only a small fraction of used tires was reused in the form of energy or materials (Aiello et al., 2009). Over the past 15 years, waste management of exploited tires has become a key concern for many environmental bodies and agencies (especially in the EU where in 2003 the disposal of tires to landfill was prohibited and in 2006 the disposal of tire by-products to landfill was prohibited) (Neocleous et al., 2011). Very demanding European environmental legislation forced European states and tire industry to significantly change waste management of used tires (Achilleos et al., 2011). New facilities dedicated to recycling of exploited

* Corresponding author.

E-mail address: jacek.katzer@yahoo.com (J. Katzer).

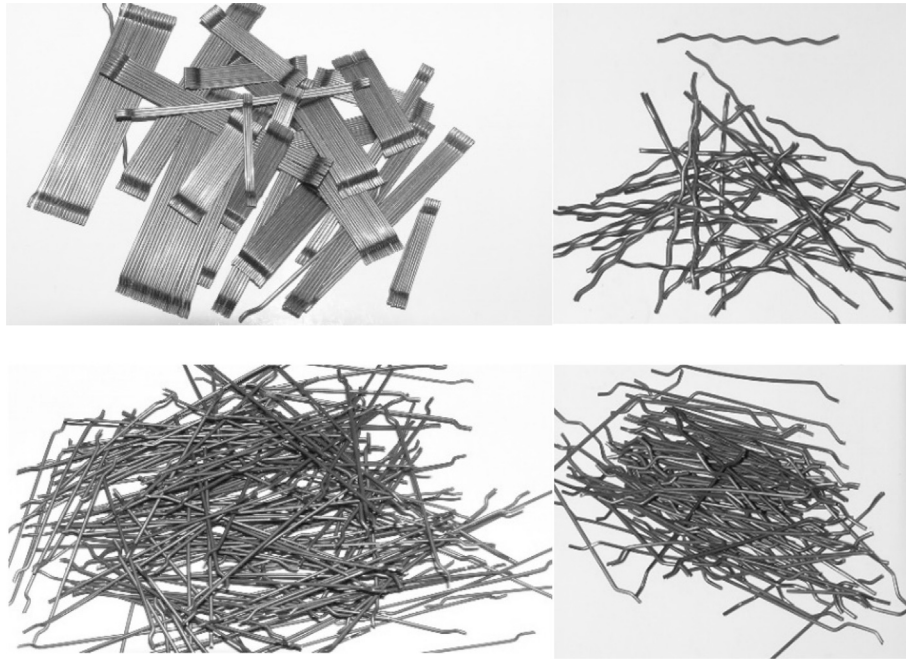


Fig. 1. Examples of geometric shapes of commonly used ESFs.

tires were created all over Europe. Initially, material recovery (rubber and steel) from used tires was done mechanically (Angelakopoulos, 2011). The steel in tires is in the form of belts running longitudinally around the perimeter of the tires. The steel belts are made of thin steel wires with high carbon content, which are woven together into thicker cords. The steel wires have different configurations, but all are brass coated (Baranowski et al., 2016). The cords are then woven again to form larger sheets of braided steel. These sheets are sandwiched between two layers of rubber (Torretta et al., 2015). Most tires contain two or three steel belts. An ordinary light vehicle tire consists of 15% of steel by weight. Average truck tires contain up to 25% of steel by weight (Graeff, 2011). This complex internal structure is difficult to recycle mechanically. Early recycling facilities utilizing mechanical material recovery were “producing” long steel wires tangled together forming a three-dimensional mesh, which could not be used as RFC apart from slurry infiltrated concrete (SIFCON) and roller compacted concrete (Graeff et al., 2012). The fibers were also significantly contaminated by rubber parts, which influenced the overall performance of achieved SFRC. Modern state-of-the-art tire recycling facilities are based on thermal degradation process. During the process, tires are reduced to steel, char, liquids, and gases (Graeff, 2011). The achieved steel fiber is clean (with no rubber contamination), and its availability grows significantly due to new recycling facilities being open all over the world. Assuming the 100% tire recycling rate, there would be more than 500 000 tons of recovered steel fiber in the EU alone (Pilakoutas et al., 2004). This amount of WSF would cover the whole current global consumption of ESF with 50% surplus margin. In a very near future, harnessing all available WSFs will become a major problem. Using WSF as concrete reinforcement is no longer limited by fiber availability or poor quality but by competition with ESF. Full knowledge about the mechanical properties of WSFs is required (Bartolac et al., 2016) to efficiently compete with ESF and eventually fully substitute them on the market. Research programs dealing with WSF and conducted in previous years were mainly focused on the properties of the achieved SFRC. The properties of fiber (both ESF and WSF), apart

from some geometrical dimensions, were omitted in this research and theoretical analysis. In authors' opinion, thorough knowledge about fiber properties is essential for achieving high-performance SFRC. The more sophisticated and demanding applications found for SFRC, the more thorough knowledge about fiber properties needed. The bond between steel fiber and concrete matrix is crucial for maintaining specific mechanical properties of SFRC (Graeff et al., 2011). Fiber can be either pulled out from the matrix or destroyed if the bond with the matrix is strong enough. Therefore, fiber's geometrical properties (defining its external surface and hook efficiency) are so important for achieving high mechanical performance of SFRC. Fiber tensile strength and tensile strength after bends influence multiple SFRC properties including dynamic response and fatigue durability. Mechanical and geometrical characteristics of a steel fiber define the overall quality of the achieved SFRC (Katzer and Domski, 2012). Nevertheless, the mechanical characteristics of fiber are underestimated and neglected in ordinary SFRC designing. Keeping in mind all the above facts, the authors decided to conduct a research program focused on the mechanical characteristics of the most popular ESF and WSF. The comparison of these properties would enable efficient and technically viable use of WSF for SFRC production. Modeling and feasible SFRC mix designing are based on these data too. The most efficient utilization of both types of fiber reinforcement would also be enabled. This paper initially presents the ESF and WSF chosen for the study. It is followed by a description of testing methodology and research program. The main results are presented in the form of stress–strain relations after bends. The paper concludes with a discussion.

2. Method section

As representatives of ESF, hooked steel fibers offered by different producers in Europe were chosen. The hooked type of ESF is the most popular on the global civil and structural engineering market (Domski, 2016). This popularity is followed by a vast number of research programs focused on the properties of SFRC

based on hooked ESF (Zollo, 1997). Therefore, the influence of the addition of this type of fibers on the properties of ordinary concrete, self-compacting concrete, and concrete based on waste aggregates is thoroughly described in numerous scientific publications (Belferrag et al., 2016). Any new ESF or WSF entering the civil engineering market would have to compete with the hooked ESF (Pajak and Ponikiewski, 2013). Thus, comparing the properties of WSF in question with the properties of different hooked ESFs is so essential for successful harnessing of the WSF. SFRC with hooked fiber is successfully used for industrial floors, road and airport pavements, precast elements, marine structures, tunneling, blast resistant structures, and earthquake-resistant structures (Ponikiewski et al., 2014). Therefore, hooked ESF seems to be the best reference point for the properties of WSF (Guoa et al., 2014).

ESFs offered by main global producers are characterized by the aspect ratio of 20–152. Fibers characterized by the aspect ratio of 50 are statistically the most popular group of ESF in the world (Katzner and Domski, 2013). That is why seven hooked ESF types characterized by the aspect ratio of 50–80 were chosen for the tests, as a precise representation of commonly used ESFs (Domski, 2015). All the types of ESF were made of cold drawn wire (Group I in compliance with EN 14889-1:2009). Some properties of these fibers were described and discussed in a previous publication (Katzner and Domski, 2012). Geometric characteristics of these fibers are presented in Table 1.

WSF was sourced from the newly opened tire recycling facility located in Rożental (Poland). The facility was chosen as one of the most modern in Europe and “producing” steel fiber free from any rubber contamination. It is available as a mix of fibers differentiated by diameter (from 0.15 mm to 0.35 mm) and length (from 10 mm to 70 mm). Fibers characterized by diameter smaller than 0.24 mm are present only in a small fraction and were rejected from the tests as outliners. Before testing, WSFs were sorted and divided into two groups. Group I consisted of fibers characterized by diameter from 0.24 mm to 0.29 mm and was coded as “I – 0.29÷0.24.” Group II consisted of fibers characterized by diameter from 0.30 mm to 0.35 mm and was coded as “H – 0.35÷0.30.” Raw WSFs obtained from recycling facility and both fiber groups separated from them are presented in Fig. 2 (only fibers with length larger than 30 mm were considered for tests). The aspect ratio of WSF was ranging from 28.6 to 291.7. Diameter distribution of both tested WSFs is presented in Fig. 3 and summarized in Table 2.

Both WSF populations are characterized by negative skewness (relatively high). In case of fiber diameter, negative skewness is the desired population characteristic. It means that the distribution is concentrated on the right side of the figure, the left tail is longer, and there are few low values. The population of fiber H – 0.35÷0.30 is characterized by nearly zero excess kurtosis, whereas the population of fiber I – 0.29÷0.24 is characterized by positive excess kurtosis; thus, fiber populations should be considered as *mesokurtic* and *leptokurtic*, respectively. Leptokurtic distribution also known as

super Gaussian distribution is the most desirable in case of fiber population characteristics.

The research program covered the tests of tensile strength of fiber and fiber ductility. The tensile strength test was conducted according to EN ISO 6892-1:2009. The test is characterized by a constant rate of increase of the loading force. During the tensile strength test, the full strain–stress relation was followed and recorded. The ductility test was realized on the end diameter before deformation according to EN 10218-1:1994 (this procedure is also described in ISO 7801:1984). During the test, a mounted fiber is bent over a cylindrical support. The radius of the support depends on the fiber diameter and ranges from 1.25 mm to 2.5 mm. A photograph of the used apparatus with a mounted fiber and a schematic diagram of fiber being bent during the test are presented in Fig. 4.

After each bend, the tensile strength of fiber was tested. Both tests were conducted on the population of 30 fibers. The randomness of fiber sampling was ensured by using the table of random numbers. The whole test procedure is as follows: 30 fibers were tested for tensile strength, 30 fibers were bent once and then tested for tensile strength, and 30 fibers were bent twice and then tested for tensile strength *et cetera*. In this way, to get results for one fiber type after seven bends, 240 fibers were used. The procedure was conducted under strict statistical control. Dixon's Q test and Kolmogorov–Smirnov test (Corder and Foreman, 2009) were utilized for identification (and rejection) of outliners and for assessment of normal (Gaussian) distribution in all achieved populations of results, respectively.

3. Achieved results

The tensile strength of ESF declared by producers should range from 800 MPa to 1250 MPa. The number of bends for these types of fiber should be at least seven. Tensile strength requirements were fulfilled by all tested ESFs. In case of a minimum number of bends, fiber B-1.00 and E-0.80 did not achieve the needed values. The tensile strength of tested fiber after bends is presented in Fig. 5. All fitted equations are linear functions. In case of ESF, the correlation factor r ranged from 0.95 for fiber D – 0.90 to 0.97 for fiber A – 1.00. Linear functions for WSF were fitted with much smaller correlation factor r , which was equal to 0.75 for fiber I – 0.29÷0.24 and 0.10 for fiber H – 0.35÷0.30. The number of bends after which ESF failed ranged from 5 (E – 0.80) to 10 (G – 0.55). All ESFs lost their tensile strength after each bending. The tensile strength of ESF after the maximum number of bends before failure is lower by 15%–32% from the “original” strength. The decline of tensile strength after each bend takes place at a constant rate for all ESFs and is not directly associated with the diameter of tested fiber or the maximum number of bends. The largest loss of tensile strength was registered for fiber A – 1.00 (32% after seven bends), but the second largest loss was registered for fiber E – 0.80 (27% after five bends).

Table 1
Geometric characteristics of tested fibers.

	Fiber type	l (mm)	d (mm)	l/d (–)	Cross section	Producer	Code name
Fiber 1	ESF	50	1.00	50.0	Circular	A	A – 1.00
Fiber 2	ESF	50	1.00	50.0	Circular	B	B – 1.00
Fiber 3	ESF	60	1.00	60.0	circular	C	C – 1.00
Fiber 4	ESF	50	0.80	62.5	circular	D	D – 0.80
Fiber 5	ESF	60	0.75	80.0	circular	E	E – 0.75
Fiber 6	ESF	60	0.90	66.7	circular	F	F – 0.90
Fiber 7	ESF	30	0.55	54.5	circular	G	G – 0.55
Fiber 8	WSF	10÷70	0.35÷0.30	28.6÷233.3	circular	H	H – 0.35÷0.30
Fiber 9	WSF	10÷70	0.29÷0.24	34.5÷291.7	circular	I	I – 0.29÷0.24

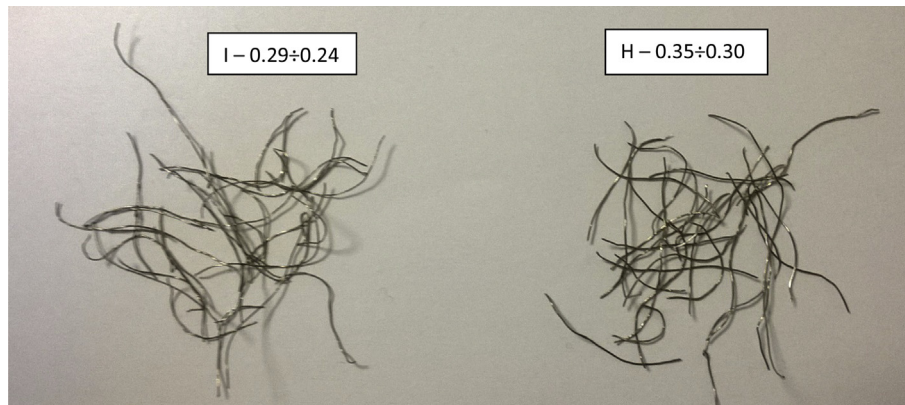


Fig. 2. WSFs acquired from the recycling facility and sorted into two groups.

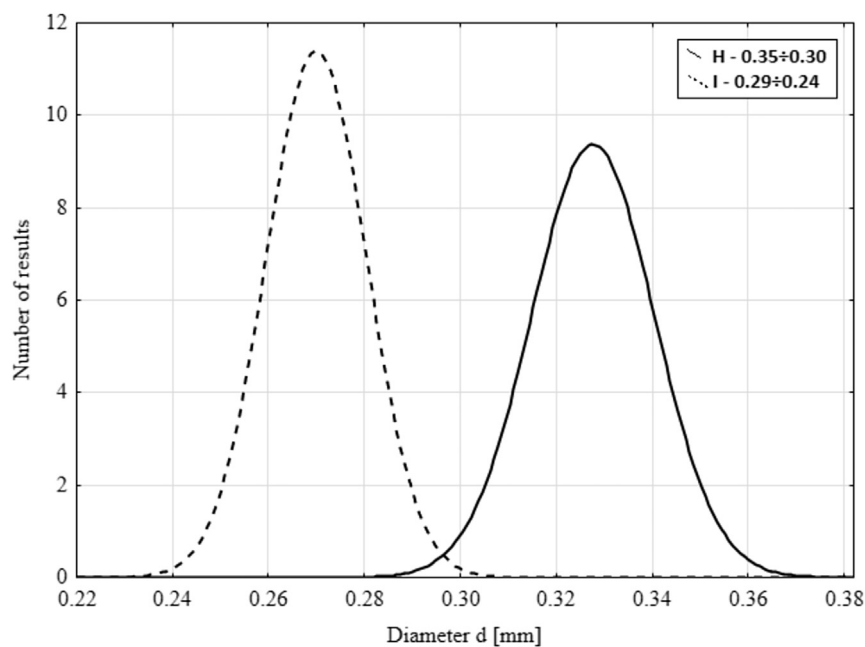


Fig. 3. Fiber diameter distribution of both tested WSFs.

Table 2
Statistical characteristics of WSF diameter.

	Median	Lower quartile	Upper quartile	Skewness	Kurtosis	Test K-S
H – 0.35±0.30	0.33	0.32	0.34	–0.38	–0.07	0.172
I – 0.29±0.24	0.27	0.26	0.28	–0.76	1.12	0.233

The smallest loss of tensile strength taken place after eight bends of fiber D – 0.90 and was equal to 15%.

The relationship between the number of bends and the tensile strength is very different in case of WSF. Both tested WSFs are characterized by much larger ductility (equal to 25 and 31 bends) than any of the tested ESFs. The graphical representation of ductility test in Fig. 5 was only prepared for the first 20 bends. Statistical characteristics of ductility distributions of WSF are presented in Table 3 and Fig. 6. The tensile strength of ESF seems to be not influenced by bending. While analyzing Fig. 5, one has to remember that linear functions fitted for WSF relations are characterized by much lower values of correlation coefficient *r*.

Therefore, the almost horizontal layout of the relation for fiber H – 0.35±0.30 and the slightly increasing tendency of tensile strength after bends of relation for fiber I – 0.29±0.24 should be analyzed with adequate reservations.

In comparison with ESFs that lose up to 50% of the initial tensile strength after the maximum number of bends (usually from seven to eight), WSFs are very resistant to the process. Maintaining the initial value of the tensile strength regardless of the number of conducted bends is a new property, so far not recognized by standards describing steel fiber. This new mechanical characteristic, not achieved by ESF, is very important in case of fibers foreseen to be used in concrete structures prone to all kinds of dynamic

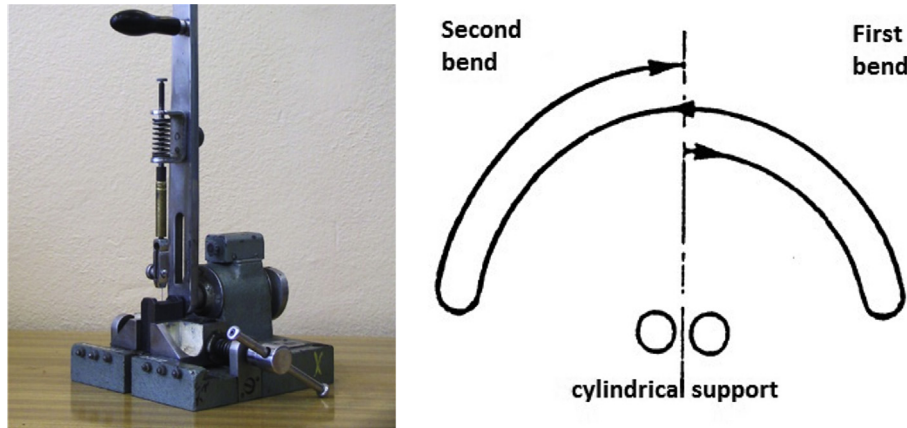


Fig. 4. Utilized ductility apparatus (left) and diagram of fiber being bent during the test (right) (Katzer and Domski, 2012).

loadings.

The presented stress–strain curves were achieved through direct testing of fibers. The length of the fiber and its diameter are much smaller than the size of the standard round bar specimen used for tensile testing of steel. Therefore, the achieved stress–strain relations of fiber cannot be directly compared with the characteristics of steel specimens and any standard requirements regarding steel as a material. Nevertheless, the charts presented in Figs. 7–9 are worth analyzing for drawing some conclusions. In case of all tested ESFs but one, presented curves show the stress–strain relation of structural steel with clear proportional limit and yield point. Using the yield point as an assessment tool of mechanical characteristic of ESFs, one can divide fibers into three groups. Group I consists of fiber A – 1.00, C – 1.00, and D – 0.90 characterized by unchanged location of the yield point (roughly the same value of strain) regardless of the number of conducted bends. Group II consists of fiber B – 1.00, E – 0.80, and F – 0.75 characterized by changing location of the yield point. The number of conducted bends significantly moves the yield point to much higher values of strain. Group III consists of fiber G – 0.55 characterized by the stress–strain relation with no or very blurred yield point. Bends significantly influence the characteristics of almost all tested ESFs making the relations more flat (smaller stress needed for creating the same strain) after every bend. This phenomenon is clearly visible in five types of ESF. In case of the two types of ESF (C – 1.00 and D – 0.90), only the stress–strain curve for the fiber with no bends is different from the others. The relationships created after the first and subsequent bends form a dense population of curves which are impossible to distinguish. These two types of ESFs are also characterized by the same number of conducted bends (equal to eight). Stress–strain curves created for WSF are significantly different from the relations achieved for ESF. Larger strains for small stresses were caused by straightening of WSF in the beginning of the test. The majority of the curves' lengths could be classified as elastic region with no visible yield stress or plastic region. In both WSF cases, conducted bends significantly influence the stress–strain relation making them less steep. Ultimate strains reach over 10% and 12% for fibers I – 0.29±0.24 and H – 0.35±0.30, respectively.

4. Discussion

The strain values of ESF are much higher than one would have expected from the steel type and values of the modulus of elasticity declared by producers. This phenomenon can be explained by straightening a fiber during the tensile strength test. Hooked fibers

are in theory straight, but in practice they are usually slightly crescent. The second factor influencing the strain values is deformation of fiber during the ductility test. After one full bend, the shape of a fiber is locally deformed. This deformation is straightened during the initial phase of the tensile strength test. A similar situation takes place while testing WSF. These fibers are not straight at all before tests. They are deformed and micro-bent multiple times over the whole length. During the ductility test, the initial deformation of fiber influences the strain values which are twice as large as in case of ESF. There are also significant differences in general shape of stress–strain curves of ESF and WSF. This phenomenon is associated with different types of steel used for the production of ESF and steel belts in tires. The properties of steel result from both its chemical composition and its method of manufacture, including processing during fabrication. Steel used for production of ESF is characterized by smaller ultimate tensile strength, smaller ductility, and yield strength. Following the changes of stress–strain curves after bends, one can assume that the modulus of elasticity E of all tested fibers would change with a number of conducted bends. The values of E would drop by two-thirds in some cases (B – 1.00 and G – 0.55). However, fibers C – 1.00 and D – 0.90 maintained almost unchanged stress–strain characteristics after all conducted bends influencing the value of E by <10%. Changes in the modulus of elasticity of WSF are much more challenging to assess due to large initial strains and varying leaning of curves after conducted bends.

The stress–strain characteristics of fiber G – 0.55 are very different from the characteristics of other ESFs. It may raise questions about the type and quality of steel used for production. The characteristic of ESFs after bends is quite similar to that of WSFs. Taking into account the largest number of conducted bends (in comparison with other tested ESFs), the mechanical characteristics of these fibers are placed between ESFs and WSFs.

The properties of WSFs are utilized as concrete reinforcement. WSFs do not have hooks that increase the force needed for fiber pullout (Kim et al., 2008), but the diameter of fiber is smaller. Thus, one volume unit of WSFs has much higher total external surface than that of ESFs. Therefore, the effect of hook would be at least partially suppressed by much higher surface bond. A comparison of pullout test results of ESFs and WSFs should be conducted to precisely describe this phenomenon (Soetensa et al., 2013). However, significantly higher tensile strength and tensile strength after bends of WSF than of ESF give more chance for future improvement of SFRC. Elements prone to different types of dynamic loadings are the first choice of application of such fibers. Apart from very high ductility and tensile strength after bends, the used steel is also

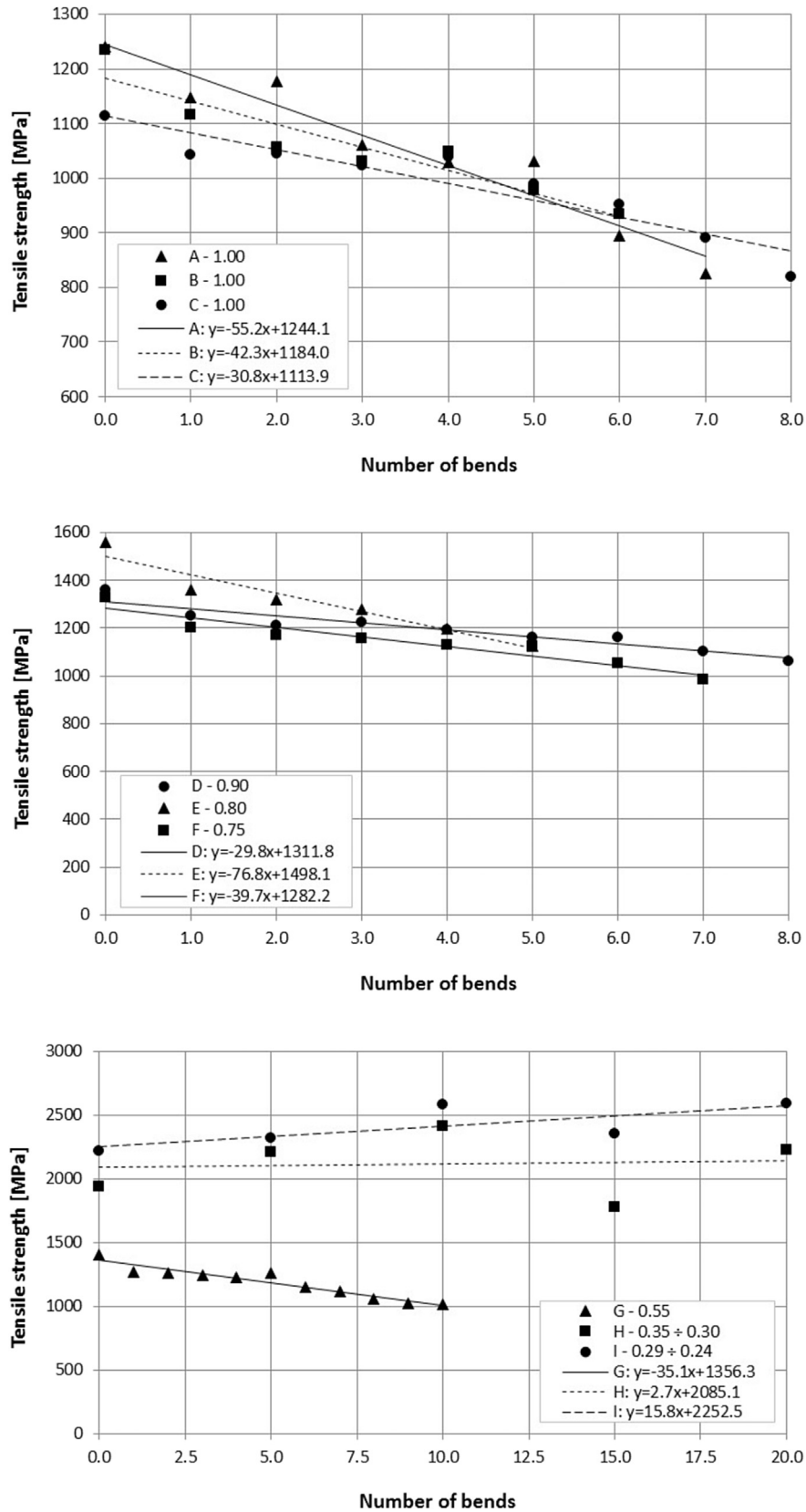


Fig. 5. Tensile strength of fiber after bends.

characterized by much higher resistance to the corrosion. In case of dynamically loaded SFRC structures, one has to face a problem of multiple small cracks appearing on the surface (Sucharda et al.,

2015). Water easily penetrates through these cracks and triggers corrosion of ESF, which leads to failure of the whole element. SFRC based on WSF would be much more resistant to such a process. A

Table 3
Statistical characteristics of ductility distributions.

	Median	Lower quartile	Upper quartile	Skewness	Kurtosis	Test K-S
H – 0.35±0.30	25.0	11.0	34.0	0.46	–0.51	0.106
I – 0.29±0.24	31.5	16.0	42.0	–0.19	–1.21	0.150

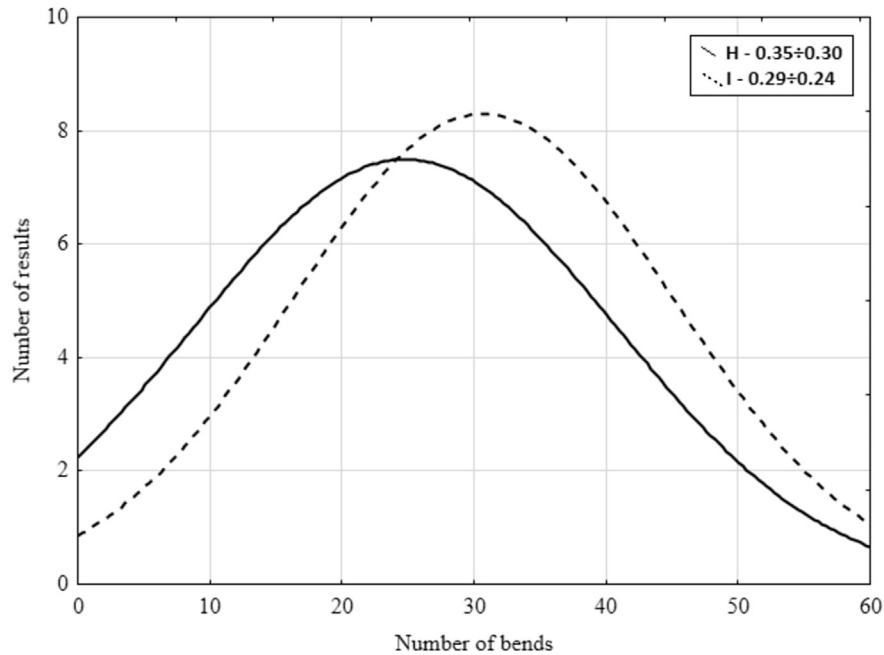


Fig. 6. Ductility of tested steel fibers.

new approach to designing such SFRC would be also needed taking into account a different bond between such fiber and concrete matrix because of steel type and geometrical properties (Soulioti et al., 2011).

The executed research program provided some knowledge about the crucial properties of WSF obtained from recycling of tires. A thorough knowledge about geometry, tensile strength, and ductility enables precise designing and modeling (Colajanni et al., 2012) of SFRC created with this fiber. Harnessing fiber characterized by higher tensile strength and much higher ductility than traditional ESF gives an opportunity to compose high-performance SFRC dedicated to bear harmonic loading, fatigue loading, impact loading, blast loading, and other incidental dynamic loadings (Biolzi and Cattaneo, 2017). Possibly, the most important type of SFRC with respect to WSF would be concrete created on the basis of waste aggregates (Łapko and Grygo, 2016). So far, such concretes have been reinforced by ESFs (Pastorellia and Herrmann, 2016). Using WSFs instead of ESFs would further increase sustainability and decrease carbon footprint of such concretes (Senaratne et al., 2016). During the research program, WSFs were compared with hooked ESFs. This type of ESFs as the most popular type of steel fibers available on the global civil engineering market was chosen as a reference for the properties of WSFs. Short ESFs are rarely used and relatively difficult to obtain (Jian-he et al., 2015). Nevertheless, comparing the properties of WSFs with those of ESFs of similar lengths would be interesting and beneficial for the development of sustainable SFRC.

5. Conclusions

The properties of ESFs and WSFs were investigated and

compared in this study. Tested ESFs proved to be much more diverse than the commonly assumed fibers. The aspect ratio and other geometrical properties are not associated with changes in the mechanical characteristics of ESFs. More properties of ESFs should be tested and analyzed at the same time (preferably using multivariate statistics) to get clear correlations. The type and quality of steel used by particular ESF producers may be one of the key underestimated factors. So far, the properties of ESFs were recognized as much dominant over the properties of concrete matrix that no research effort was dedicated to thoroughly evaluate them.

The properties of both WSF populations are similar and their application for a particular concrete would be limited only by geometrical requirements. Stress–strain characteristics of ESF and WSF differ significantly. This phenomenon is mainly caused by different types of steel used for the production of ESF and steel used for tire production. The type of steel also influences other mechanical properties of WSF such as tensile strength and ductility. WSF is characterized by much higher tensile strength and ductility than ESF. Conducted bends influence the tensile strength and modulus of elasticity of all tested fibers, but WSF is ultimately destroyed after up to three times more bends than ESF. Fibers C – 1.00 and D – 0.90 are the least prone to changes in stress–strain characteristics after bends. Fibers B – 1.00 and G – 0.55 are the most vulnerable to changes of stress–strain relation after bends. Stress–strain relations of both tested types of WSFs have different geometric characteristics in comparison with ESF. This phenomenon is partially caused by the type of steel and partially by initial geometric deformations of WSF. During tensile test, the first part of the stress–strain relation reflects the straightening of WSF. Overall strain of ESF and WSF after five bends is similar. For ESF, strains after 6–10 bends are ultimate due to specimen failure. From the

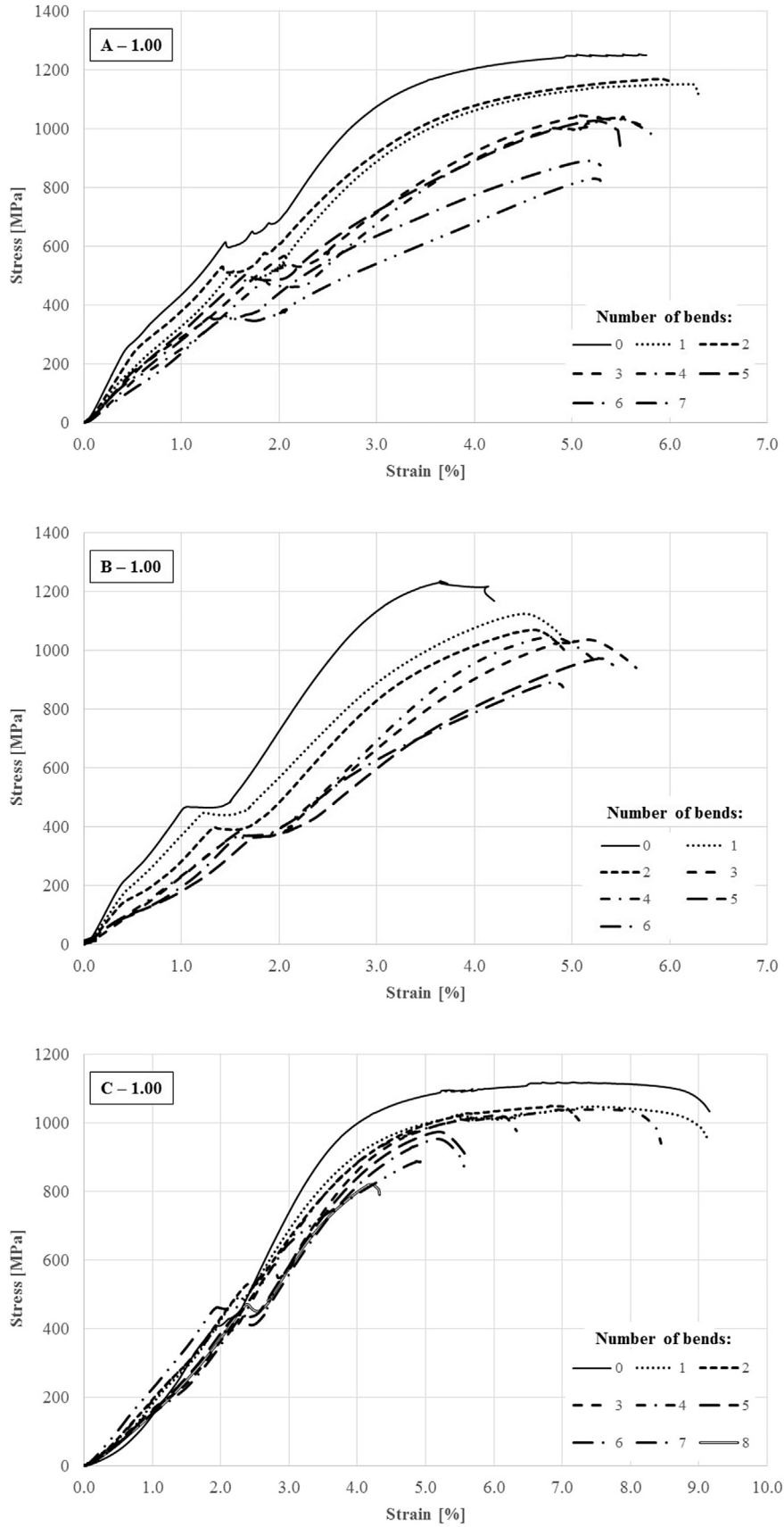


Fig. 7. Stress–strain relations after bends for ESF with a diameter of 1 mm.

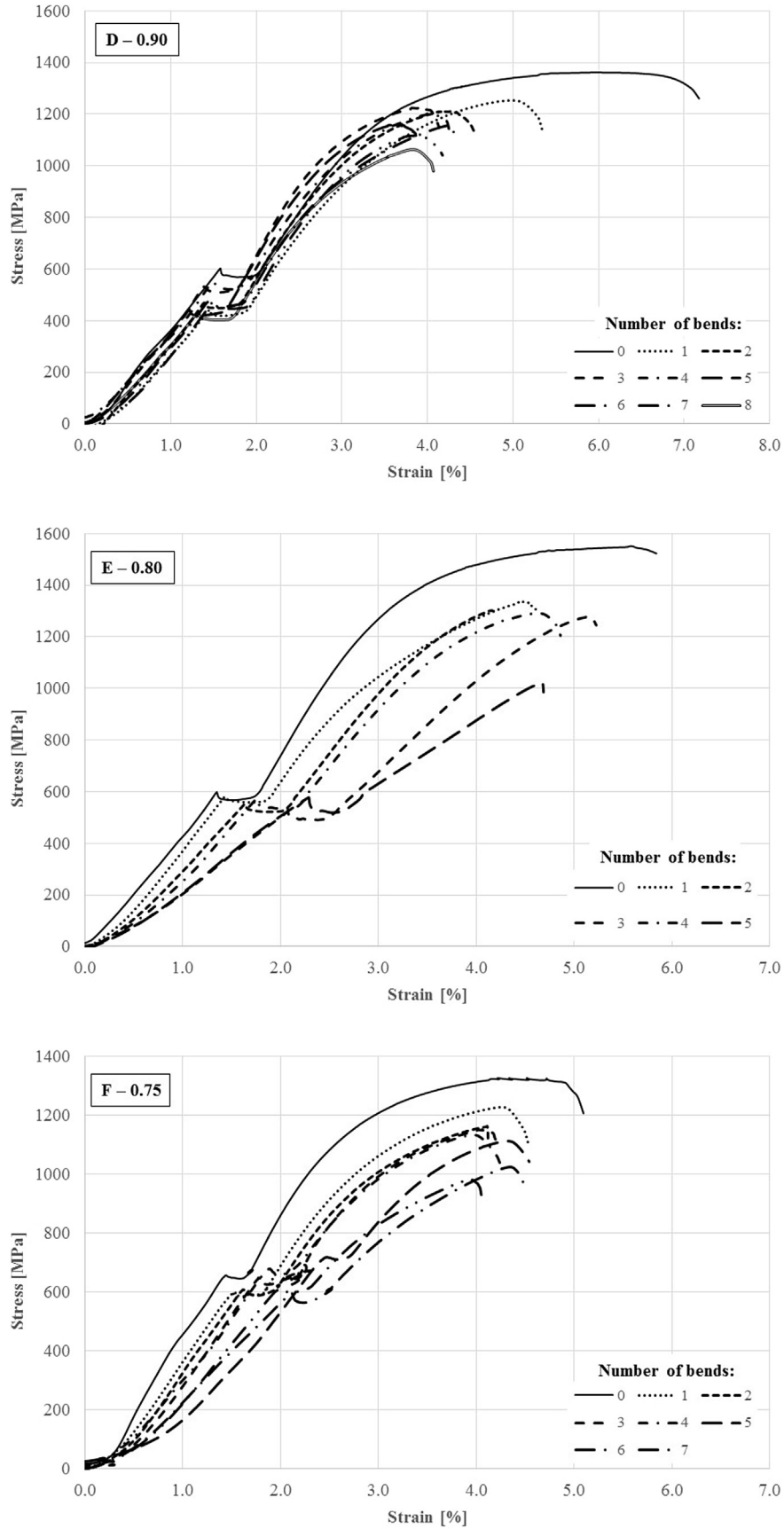


Fig. 8. Stress–strain relations after bends for ESF with a diameter of <1 mm.

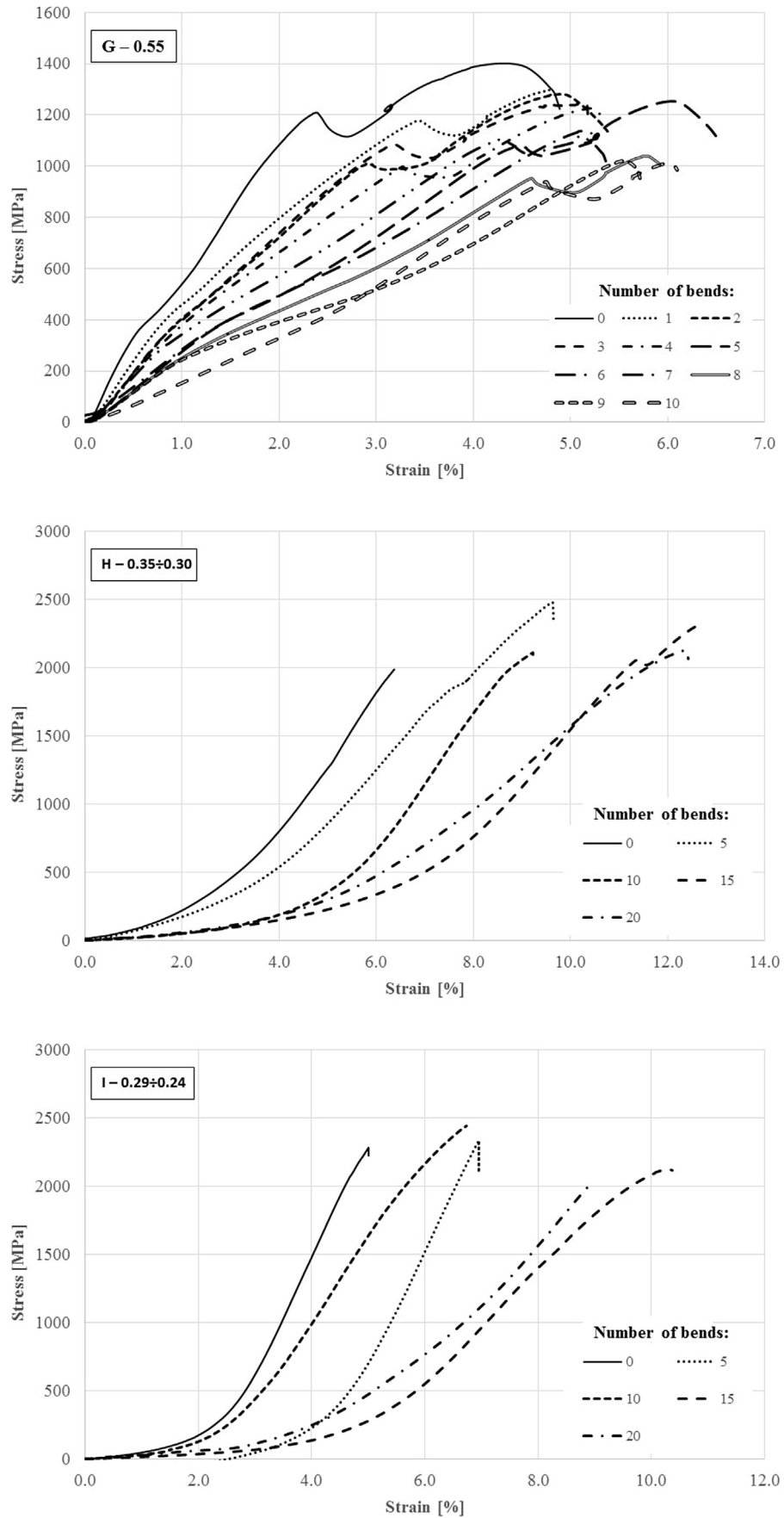


Fig. 9. Stress–strain relations after bends for ESF G – 0.55 mm and both WSFs.

mechanical and the geometrical point of view, WSF can be used as concrete reinforcement. Due to its high ductility and stress–strain characteristics after bends, WSF gives an opportunity to compose an efficient SFRC dedicated to bear harmonic loading, fatigue loading, impact loading, and blast loading. Keeping in mind that WSF is made of different types of steel than ESF and the lack of hooks (or deformed ends), a pullout test of WSF should be conducted. The achieved results should be compared with the pullout characteristics of ESF. Before harnessing WSF on an industrial scale in concrete industry, a possible chemical contamination of the WSF should be tested to be sure whether it is safe to use as concrete reinforcement. It would be beneficial to test short and very short ESFs and compare their properties with WSFs. A research program comparing the properties of SFRC with respect to ESF and WSF should be conducted.

References

- Achilleos, C., Hadjimitsis, D., Neocleous, K., Pilakoutas, K., Neophytou, P., Kallis, S., 2011. Proportioning of steel fibre reinforced concrete mixes for pavement construction and their impact on environment and cost. *Sust* 3, 965–983.
- Aiello, M.A., Leuzzi, F., Centonze, G., Maffezzoli, A., 2009. Use of steel fibres recovered from waste tyres as reinforcement in concrete: pull-out behaviour, compressive and flexural strength. *Waste Manag.* 29 (6), 1960–1970.
- Angelakopoulos, H., 2011. *Recycled Steel Fibre Reinforced Roller-compacted Concrete* (PhD Thesis). The University of Sheffield, Sheffield, UK.
- Baranowski, P., Malachowski, J., Janiszewski, J., Wekezer, J., 2016. Detailed tyre FE modelling with multistage validation for dynamic analysis. *Mater. Des.* 96, 68–79.
- Bartolac, M., et al., 2016. Punching shear strength of concrete slabs reinforced with recycled steel fibres from waste tires. In: *Proceedings of II International Conference on Concrete Sustainability (ICCS16)*, Barcelona, Spain.
- Belferrag, A., et al., 2016. Effect of granulometric correction of dune sand and pneumatic waste metal fibers on shrinkage of concrete in arid climates. *J. Clean. Prod.* 112, 3048–3056.
- Biolzi, L., Cattaneo, S., 2017. Response of steel fiber reinforced high strength concrete beams: experiments and code predictions. *Cem. Concr. Compos.* 77, 1–13.
- Colajanni, P., Recupero, A., Spinella, N., 2012. Generalization of shear truss model to the case of SFRC beams with stirrups. *Comput. Concr.* 9, 227–300.
- Corder, G.W., Foreman, D.I., 2009. *Nonparametric Statistics for Non-statisticians: a Step-by-step Approach*. Wiley, New Jersey, USA.
- Domski, J., 2015. Long-term study on fibre reinforced fine aggregate concrete beams based on waste sand. *Rocz. Ochr. Sr.* 17, 188–199.
- Domski, J., 2016. A blurred border between ordinary concrete and SFRC. *Constr. Build. Mater.* 112, 247–252.
- EN 10218-1:1994. Steel wire and wire products. General. Test methods.
- EN 14889-1:2009. Fibres for concrete - Part 1: Steel fibres - Definitions, specifications and conformity.
- EN ISO 6892-1:2009. Metallic materials – Tensile testing – Part 1: Method of test at room temperature.
- Ghorpade, V.G., Sudarsana Rao, H., 2010. Strength and permeability characteristics of Fibre reinforced recycled aggregate concrete with different fibres. *Nat. Environ. Pollut. Technol.* 9, 179–188.
- Graeff, A., 2011. *Long Term Performance of Recycled Steel Fibre Reinforced Concrete for Pavement Applications* (PhD Thesis). The University of Sheffield, Sheffield, UK.
- Graeff, A., Vania, M., Peres, N.N., Silva-Filho, L.C.P., Neocleous, K., Pilakoutas, K., 2011. Use of recycled steel fibres recovered from post-consumer tyres as fatigue reinforcement for concrete pavements. In: *Proceedings of the Second International Conference on Best Practices for Concrete Pavements*, Florianopolis, Santa Catarina, Brazil, 2–4 November 2011.
- Graeff, A.G., Pilakoutas, K., Neocleous, K., Peres, M.V.N.N., 2012. Fatigue resistance and cracking mechanism of concrete pavements reinforced with recycled steel fibres recovered from post-consumer tyres. *Eng. Struct.* 45, 385–395.
- Guoa, Yong-chang, Zhanga, Jian-hong, Chena, Guang-ming, Xieb, Zhi-hong, 2014. Compressive behaviour of concrete structures incorporating recycled concrete aggregates, rubber crumb and reinforced with steel fibre, subjected to elevated temperatures. *J. Clean. Prod.* 72 (1), 193–203.
- Havlikova, I., et al., 2015. Effect of fibre type in concrete on crack initiation. *Appl. Mech. Mater.* 769, 308–311.
- Jian-he, Xie, et al., 2015. Compressive and flexural behaviours of a new steel-fibre-reinforced recycled aggregate concrete with crumb rubber. *Constr. Build. Mater.* 79, 263–272.
- Katzer, J., 2006. Steel fibers and steel fiber reinforced concrete in civil engineering. *Pac. J. Sci. Technol.* 7 (1), 53–58.
- Katzer, J., Domski, J., 2012. Quality and mechanical properties of engineered steel fibres used as reinforcement for concrete. *Constr. Build. Mater.* 34, 243–248.
- Katzer, J., Domski, J., 2013. Optimization of fibre reinforcement for waste aggregate cement composite. *Constr. Build. Mater.* 38, 790–795.
- Kim, D.J., et al., 2008. Loading rate effect on pullout behavior of deformed steel fibres. *ACI Mater. J.* 576–584. November–December 2008.
- Maidl, B.R., 1995. *Steel Fibre Reinforced Concrete*. Ernst & Sohn, Berlin, Germany.
- Mohammadi, Y., et al., 2008. Properties of steel fibrous concrete containing mixed fibres in fresh and hardened state. *Constr. Build. Mater.* 22, 956–965.
- Naaman, A.E., 2003. Engineered steel fibres with optimal properties for reinforcement of cement composites. *J. Concr. Adv. Technol.* 1 (3), 241–252.
- Nawy, E.G., 1996. *Fundamentals of High Strength High Performance Concrete*. Longman, England.
- Neocleous, K., et al., 2011. Fibre-reinforced roller-compacted concrete transport pavements. *ICE Proc. Transp.* 164, 97–109.
- Pająk, M., Ponikiewski, T., 2013. Flexural behavior of self-compacting concrete reinforced with different types of steel fibers. *Constr. Build. Mater.* 47, 397–408.
- Pastorellia, E., Herrmann, H., 2016. Time-efficient automated analysis for fibre orientations in steel fibre reinforced concrete. *Proc. Est. Acad. Sci.* 65 (1), 28–36.
- Pilakoutas, K., Neocleous, K., Tlemat, H., 2004. Reuse of tyre steel fibres as concrete reinforcement. *Proc. Inst. Civ. Eng. Eng. Sustain.* 157 (ES3), 131–138.
- Ponikiewski, T., et al., 2014. Determination of steel fibres distribution in self-compacting concrete beams using X-ray computed tomography. *Arch. Civ. Mech. Eng.* <http://dx.doi.org/10.1016/j.acme.2014.08.008>.
- Senaratne, S., Gerace, D., Mirzac, O., Tamc, V.W.Y., Kangd, Won-Hee, 2016. The costs and benefits of combining recycled aggregate with steel fibres as a sustainable, structural material. *J. Clean. Prod.* 112 (Part 4, 20), 2318–2327.
- Soetensa, T., Van Gyselb, A., Matthysa, S., Taerwea, L., 2013. A semi-analytical model to predict the pull-out behaviour of inclined hooked-end steel fibres. *Constr. Build. Mater.* 43, 253–265.
- Soulioti, D.V., Barkoula, N.M., Paipetis, A., Matikas, T.E., 2011. Effects of fibre geometry and volume fraction on the flexural behaviour of steel-fibre reinforced concrete. *Strain Int. J. Exp. Mech.* 47, 535–541.
- Spinella, N., 2013. Shear strength of full-scale steel fibre-reinforced concrete beams without stirrups. *Comput. Concr.* 11, 365–382.
- Sucharda, O., et al., 2015. Finite element modelling and identification of the material properties of fibre concrete. *Procedia Eng.* 109, 234–239.
- Torretta, V., et al., 2015. Treatment and disposal of tyres: two EU approaches. A review. *Waste Manag.* 45, 152–160. November 2015.
- Zollo, R.E., 1997. Fibre-reinforced concrete: an overview after 30 years of development. *Cem. Concr. Compos.* 19, 107–122.
- Lapko, A., Grygo, R., 2016. Improving the structural behaviour RC precast concrete beams made of recycled aggregate concrete. *J. Civ. Eng. Manag.* 22 (2), 234–242.